Available online at www.sciencedirect.com
SCIENCE DIRECT®
International Journal of Solids and Structures 42 (2005) 1443–1463
INTERNATIONAL JOURNAL OF SOLIDS and STRUCTURES
www.elsevier.com/locate/ijsolstr

On the non-linear high-order theory of unidirectional sandwich panels with a transversely flexible core

Yeoshua Frostig [a,*], Ole Thybo Thomsen [b], Izhak Sheinman [a]

[a] *Faculty of Civil and Environmental Engineering, Technion-Israel Institute of Technology, Haifa 32000, Israel*
[b] *Institute of Mechanical Engineering, Aalborg University, Pontoppidanstræde 101, DK-9220 Aalborg, Denmark*

Received 18 May 2004; received in revised form 17 August 2004
Available online 13 October 2004

Abstract

The paper presents a general geometrically non-linear high-order theory of sandwich panels that takes into account the high-order geometrical non-linearities in the core as well as in the face sheets and is based on a variational approach. The formulation, which yields a set of rather complicated governing equations, has been simplified in two different approaches and has been compared with FEA results for verification. The first formulation uses the kinematic relations of large displacements with moderate rotations for the face sheets, non-linear kinematic relations for the core and it assumes that the distribution of the vertical normal stresses through the depth of the core are linear. The second approach uses the general formulation to the non-linear high-order theory of sandwich panels (HSAPT) that considers geometrical non-linearities in the face sheets and only linear high-order effects in the core. The numerical results of the two formulations are presented for a three point bending loading scheme, which is associated with a limit point behavior. The results of the two formulations are compared in terms of displacements, bending moments and shear stresses and transverse (vertical) normal stresses at the face–core interfaces on one hand, and load versus these structural quantities on the other hand. The results have compared well with FEA results obtained using the commercial codes ADINA and ANSYS.

Keywords: Sandwich panels; Flexible core; High-order theory; Geometric non-linearity; Localized effects; Local buckling; Limit point behavior

* Corresponding author. Tel.: +97 248293046; fax: +97 248295697.
E-mail address: cvrfros@techunix.technion.ac.il (Y. Frostig).

0020-7683/$ - see front matter © 2004 Elsevier Ltd. All rights reserved.
doi:10.1016/j.ijsolstr.2004.08.015

1. Introduction

A typical modern sandwich structure consists of two faces, made of metallic or composite laminated materials, separated by a "soft" core that is usually made of low-weight and low strength non-metallic honeycomb or polymeric foam. However, sandwich structures with such compliant/soft core materials are notoriously sensitive to large deformations, indentations and failure by the application of concentrated loads, at points or lines of support, and due to localized bending effects induced in the vicinity of points of geometric and material discontinuities. The reason for this is that, although sandwich structures are well suited for the transfer of overall bending and shearing loads, localized shearing and bending effects, as mentioned above, induce severe transverse normal and interfacial shear stresses. These stress components can be of significant magnitude, and may in many cases approach or even exceed the allowable stresses in the core material as well as in the interfaces between the core and the face sheets. In general, these localized effects are associated with large displacements and moderate rotations in the face sheets and the core, also denoted as geometrical non-linearities of the structure.

These geometrical non-linearities in a typical modern sandwich panel may consist of large displacements in the face sheets and large displacements in the core, see Fig. 1a for partially distributed loads and Fig. 1b for a concentrated load. However, since the core is located between the two face sheets its depth depends on the displacement pattern of the face sheets and on the differences of the deflections between the upper and the lower face sheets, see d_D in Fig. 1. Notice that the core, which is a two-dimensional elastic medium, exhibits large deformations in addition to an overall change of its height. However, one of the questions that can be raised about the deformed core is whether the large deformations in the core are the result of large rigid body motions of the upper and the lower face sheets (attached to the core), which implies that the core actually remains in a linear state of deformations in spite of the large deformations, or the result of large core deformations that are associated with non-linear kinematic relations. One of the major goals of this research is to examine the effects of the existence and inexistence of the geometrical non-linearities of the core, while the face sheets remain within the non-linear region, on the non-linear response of the sandwich panel.

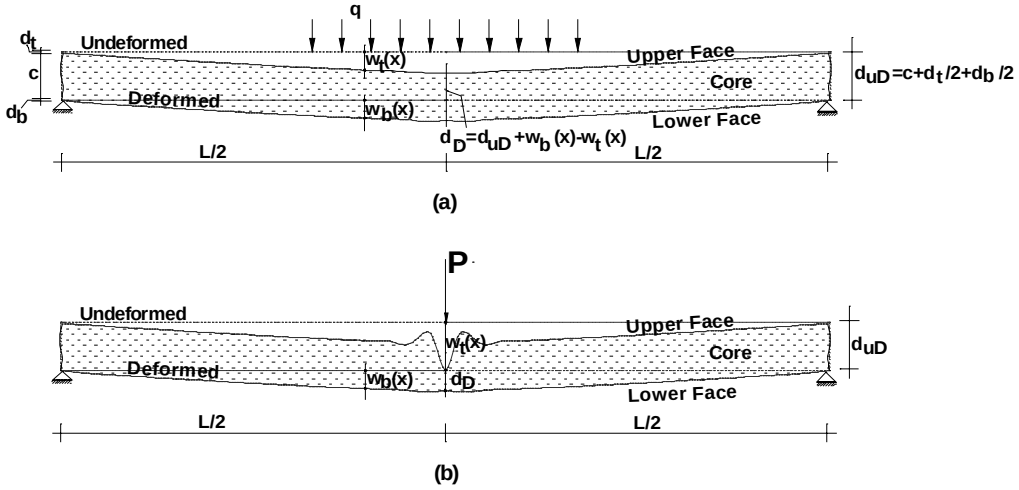

Fig. 1. Deformed shapes of sandwich panels with large deformations and moderate rotations: (a) partially distributed load—linear core, (b) a three point bending loading scheme—linear/non-linear core.

The classical analyses, linear or linearized models, see Allen (1969), Plantema (1966), Zenkert (1995), Vinson (1999) and Noor et al. (1996), for traditional sandwich panels with anti-plane cores (such as metallic honeycomb core), ignore the presence of localized effects due to the vertical flexibility of the core, and are in fact unable to detect and quantify them. In general, the approaches used for bending, overall buckling and vibration analyses, in most cases, are based on the "equivalent single layer" approach (ESL approach) in which the layered structure (of beam, plate or shell type) is replaced by a solid homogeneous panel with equivalent properties, see for example the Mindlin first-order theory (Mindlin, 1951), and Reddy's high-order theories (Reddy, 1984). Recently, Kardomateas and Huang (2003) and Huang and Kardomateas (2002) have used the ESL approach to analyse a sandwich panel with very large deformations. In these research works, Kardomateas and Haung have considered the core as a medium that only transfers shear stresses between the face sheets. They have replaced the overall sandwich panel by an equivalent panel with shear deformation capability, while the geometrical non-linearities have been ignored in their formulation. Most of the aforementioned theories disregard the changes in the height of the core (the core compressibility) and the vertical strain through the depth of the core. Hence, in such approaches, the overall panel may exhibit large displacements, while the core undergoes nearly rigid body motions with linear kinematic relations associated with small deformations.

A rational approach to investigate the effects of the vertical flexibility of the core including localized effects is to consider the sandwich panel as made of two face sheets and a core that are combined together through equilibrium and compatibility. Linear analyses of localized effects in sandwich panels, especially in the vicinity of localized and concentrated loads and supports, have been investigated by several authors including: Thomsen using an elastic foundation approach (Thomsen, 1995) as well as the chapters on localized effects in Zenkert (1995, 1997), linear elasticity solutions, see Kim and Swanson (2001) and by Frostig using an enhanced model with the High-Order Sandwich Panel Theory (HSAPT) approach, see Frostig et al. (1992). The HSAPT approach has been successfully applied to linear and nonlinear applications in the field of sandwich structures by the authors as well as by others, such as: delamination at face–core interfaces in bending of unidirectional sandwich panels, see Frostig (1992); buckling analysis of sandwich panels through linearization of the non-linear HSAPT equations, see Frostig and Baruch (1993); buckling analysis of sandwich plates through the non-linear plate equations of the HSAPT, see Frostig (1998); experimental validation and verification through photoelastic measurements, see Thomsen and Frostig (1997); analysis of the non-linear behavior of sandwich panels with rigid and non-rigid interfaces including branching behavior due to in-plane compressive loads, see Sokolinsky and Frostig (2000); special non-linear behavior, see Sokolinsky et al. (2002); comparisons of results obtained using the high-order approach, theory of elasticity and FEA results have revealed a good agreement including the correct location and regions of the localized effects, see Swanson (1999); indentation resistance failure analysis using the high-order approach, see Petras and Sutcliffe (1999, 2000); and recently an experimental and analytical study of four points bending, see Sokolinsky et al. (2003), in which the non-linear response is characterized experimentally. In a recent paper Hohe and Librescu (2003) have presented a non-linear analysis of sandwich panels and shells where the face sheets undergo large deformations with moderate rotations, and the core is assumed to remain in the linear regime with small deformations.

The literature survey reveals that the non-linear analysis of sandwich panels with incompressible cores, assume that the core remains in the regime of small deformations, i.e. that linear kinematic relations applies, although the panel as a whole undergoes large deformations. In the three-layer approach, such as the HSAPT or similar, the geometrical non-linearity is introduced only in the face sheets, while the core is assumed to remain linear. Good correlation has been observed by comparison with FEA results, see for example Swanson (1999), and experiments, see Sokolinsky et al. (2003), within the regime of small to moderate class of deformations. However, using FEA modeling to simulate a realistic sandwich panel including the very low elastic properties of the core, as compared with the face sheet, and very thin face sheets is problematic due to the large displacement and distortions of the core elements, and in many cases

the results obtained do not correlate well with reality. Hence, the development of a simplified analytical/numerical approach to solve the problems, such as the non-linear HSAPT or similar, is a necessity. Thus, the effect of the non-linearity of the core on the response should be investigated in order to verify the quality and accuracy of such solutions.

The derivation of the general non-linear governing equations is based on the following restrictive assumptions: the face sheets possess in-plane and bending rigidities; the faces and the core material undergo large displacements with small strains and remain material-wise linear; the core is considered as a 2D linear elastic continuum, where its height may change during deformation, its plane of section does not remain plane after deformation, it possesses only shear and transverse normal stiffness, whereas the in-plane (longitudinal) normal stiffness is assumed negligible due to its low rigidity compared with that of the face sheets (accordingly, the longitudinal normal stresses are assumed to be nil); and the loads are applied to the face sheets only.

The accurate model that uses the non-linear kinematic relations of large displacements and moderate rotation for the face sheets as well as the core yields a set of very complicated governing equations. The lack of a general analytical solution of the core fields requires a simplified approach that has evolved into two simplified models. Hence, the paper presents first the non-linear field equations of the accurate model panel, in a concise form, follows by the two simplified models. In the first simplified one the core is assumed to exhibits non-linear kinematic relations of the shear angle only, while in the second one the core undergoes linear kinematic relations only which also coincide with the non-linear HSAPT approach. The two models are compared numerically for a three point bending loading scheme. These results are compared, for verification, with commercial FEA code results, obtained for a sandwich panel with an isotropic or orthotropic foam cores and large displacements with large rotations. The paper ends with a summary and conclusions.

2. General non-linear analysis-field equations

The mathematical formulation of the general non-linear formulation consists of derivation of the governing field equations. They are derived through the minimization of the total potential energy that consists of the internal potential energy and the potential energy of the external loads. It reads:

$$\int_{t_1}^{t_2} \delta(U+V)\mathrm{d}t = 0 \tag{1}$$

where U and V are the internal and the external potential energies, respectively, and δ denotes the variational operator.

The first variation of the internal potential energy in terms of stresses and strains reads:

$$\delta U = \int_{V_t} (\sigma_{xxt}\delta\varepsilon_{xxt})\,\mathrm{d}v + \int_{V_b} (\sigma_{xxb}\delta\varepsilon_{xxb})\,\mathrm{d}v + \int_0^L \int_0^{c_s(x)} \int_{-b_w/2}^{b_w/2} (\tau_{xzc}\delta\gamma_{xzc} + \sigma_{zzc}\delta\varepsilon_{zzc})\mathrm{d}y\,\mathrm{d}z_c\,\mathrm{d}x \tag{2}$$

where σ_{xxj} and $\varepsilon_{xxj} (j = t, b)$ are the longitudinal normal stresses and strains in the upper and the lower face sheet, respectively; τ_{xzc} and γ_{xzc} are the vertical shear stresses and shear strains in the core; σ_{zzc} and ε_{zzc} are the normal stresses and strains in the vertical direction of the core; b_w is the width of the core; $c_s(x) = c + w_b(x) - w_t(x)$ is the height of the deformed core, where c equals the height of the undeformed core; $w_j (j = t, b)$ are the vertical displacements of the upper and the lower face sheets, respectively, see Fig. 2a; and L is the span of the panel. It should be noticed that the volume integral of the core is evaluated on the deformed shape of the core, $c_s(x)$, which is affected by the vertical displacements of the upper and lower face sheets.

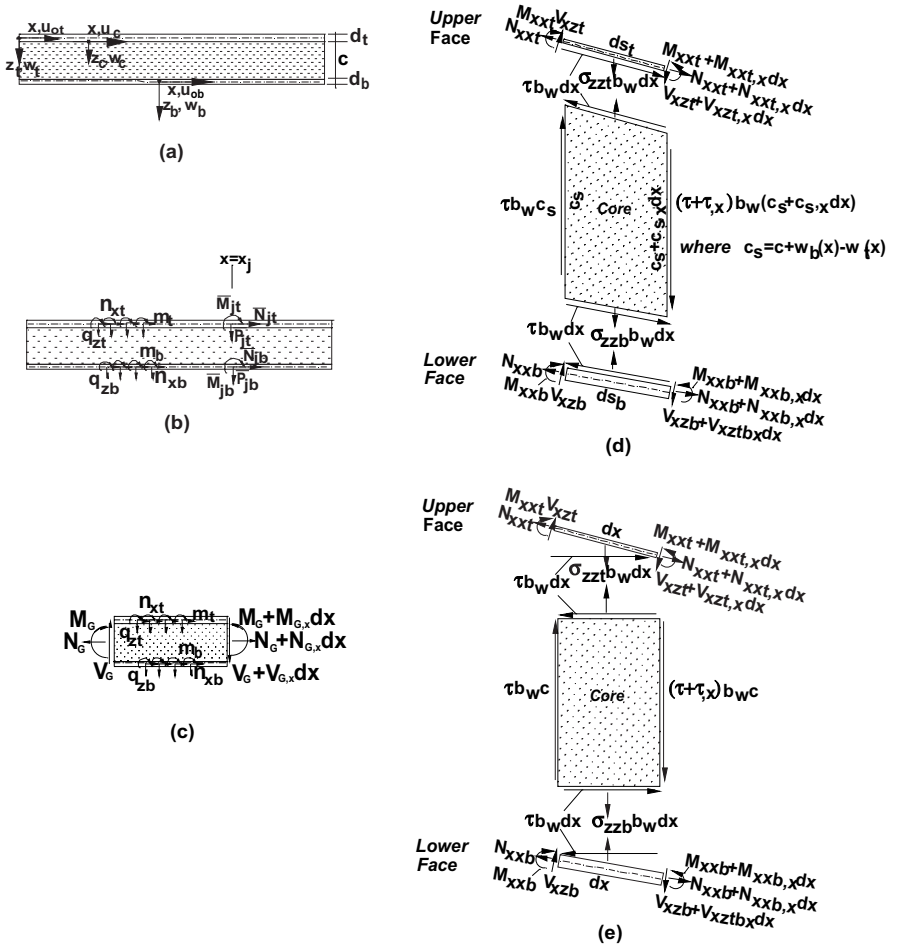

Fig. 2. Geometry, loads, internal and global stress resultants for deformed and undeformed core: (a) geometry, (b) external loads, (c) global stress resultants, (d) stress resultants with a deformed core (non-linear core), (e) stress resultants with an undeformed core (linear core).

The variation of the external work equals:

$$\delta V = -\int_0^L \Big[n_{xt}\delta u_{ot} + n_{xb}\delta u_{ob} + q_{zt}\delta w_t + q_{zb}\delta w_b + m_t\delta w_{t,x} + m_b\delta w_{b,x} + \sum_{i=0}^{Nc} \Big(\overline{N}_{it}\delta u_{ot} + \overline{P_{ib}}\delta u_{ob} + \overline{P_{it}}\delta w_t + \overline{P_{ib}}\delta w_b + \overline{M_{it}}\delta w_{t,x} + \overline{M_{ib}}\delta w_{b,x} \Big) \delta_D(x - x_{ci}) \Big] \mathrm{d}x \tag{3}$$

where u_{oj}, and $w_j (j = t, b)$ are the displacements in the longitudinal and vertical directions, respectively, of the mid-plane of the face sheets; n_{xj} and $q_{zj} (j = t, b)$ are the in-plane external loads in the longitudinal direction and the vertical distributed loads applied on the upper and lower face sheets, respectively; $m_j (j = t, b)$ are the distributed bending moments acting on the various face sheets; $\overline{N_{ji}}, \overline{P_{ji}}$ and $\overline{M_{ji}} (j = t, b)$ are the external concentrated longitudinal and vertical loads and bending moment, respectively, applied at the upper and the lower face sheets at the location $x = x_{ci}$; $\delta_D(x - x_{ci})$ is the Dirac delta function; N_c. is the number of locations with concentrated loads; $w_{j,x} (j = t, b)$ is the slope of the vertical displacement of the upper and lower face sheets, respectively. The geometry and sign convention for stresses, displacements and loads appear in Fig. 2a and b.

The kinematic relations including moderate deformations take the following form.

For the face sheets ($j = t, b$):

$$\varepsilon_{xxj} = \varepsilon_{xxoj} + z_j \chi_{xxj} \tag{4}$$

where the mid-plane inplane strains and curvatures read:

$$\varepsilon_{xxoj} = u_{oj,x} + w_{j,x}^2/2, \quad \chi_{xxj} = -w_{j,xx} \tag{5}$$

where $\varepsilon_{xxo,}$ and $\chi_{xxj}(j = t, b)$ are the in-plane strains in the longitudinal direction of the mid-plane and the curvature of the upper and the lower face sheets, respectively; z_j is the vertical coordinate of each face sheet measured downward from the mid-plane of each face sheet (see Fig. 2b), and $(\,)_{,x}$ denotes a derivative with respect to x.

The kinematic relations for the core read:

$$\gamma_{xzc} = u_{c,z_c}(x, z_c) + w_{c,x}(x, z_c) + w_{c,x}(x, z_c) w_{c,z_c}(x, z_c) + u_{c,x}(x, z_c) u_{c,z_c}(x, z_c) \tag{6}$$

$$\varepsilon_{zzc} = w_{c,z_c}(x, z_c) + \frac{1}{2} w_{c,z_c}(x, z_c)^2 + \frac{1}{2} u_{c,z_c}(x, z_c)^2 \tag{7}$$

where $u_c(x, z_c)$ and $w_c(x, z_c)$ are the longitudinal, and vertical deflections of the core, respectively, and z_c is the vertical coordinate of the core, measured downward from the upper interface (see Fig. 2b).

The compatibility conditions at the upper and the lower face–core interface, ($j = t, b$), read:

$$u_c(x, z_{cj}) = u_{oj} + \frac{1}{2}(-1)^k d_j w_{j,x}$$

$$w_c(x, z_{cj}) = w_j \tag{8}$$

where, $k = 0$ when $j = t$, and $k = 1$ when $j = b$; $z_{ct} = 0$ at the upper interface and $z_{cb} = c_s(x)$ at the lower interface (see Fig. 2a); $d_j(j = t, b)$ are the thicknesses of the upper and lower face sheets and $c_s(x)$ is the height of the core after deformation (see Fig. 2d).

The fields equations are derived through substitution of the kinematic relations, Eqs. (4)–(7) into the variation of the total potential energy, see Eq. (2), use of the stress resultants in the face sheets, see Fig. 2, and finally the compatibility conditions and equilibrium requirements between the core and the face sheets at their interfaces, see Eq. (8).

The equations for the face sheets read:

$$\begin{aligned} &-\left(\frac{\mathrm{d}}{\mathrm{d}x} N_{xxt}(x)\right) + \frac{1}{2} b_w \tau_t(x) \left(\frac{\mathrm{d}^2}{\mathrm{d}x^2} w_t(x)\right) d_t - b_w \sigma_{zzt}(x) \left(\frac{\partial}{\partial z_c} u_c(x, z_c)\right)\Big|_{z_c=0} \\ &\quad - b_w \tau_t(x) \left(\frac{\mathrm{d}}{\mathrm{d}x} u_{ot}(x)\right) - n_{xt} - b_w \tau_t(x) = 0 \end{aligned} \tag{9}$$

$$\begin{aligned} &\frac{1}{2} b_w \tau_t(x) d_t \left(\frac{\mathrm{d}^2}{\mathrm{d}x^2} u_{ot}(x)\right) + \left(\frac{\mathrm{d}}{\mathrm{d}x} m_t(x)\right) - b_w \sigma_{zzt}(x) \left(\frac{\partial}{\partial z_c} w_c(x, z_c)\right)\Big|_{z_c=0} \\ &\quad + \frac{1}{4} b_w \tau_t(x) d_t^2 \left(\frac{\mathrm{d}^3}{\mathrm{d}x^3} w_t(x)\right) - \frac{1}{2} b_w \left(\frac{\mathrm{d}}{\mathrm{d}x} \tau_t(x)\right) d_t \left(\frac{\mathrm{d}}{\mathrm{d}x} u_{ot}(x)\right) - \left(\frac{\mathrm{d}^2}{\mathrm{d}x^2} M_{xxt}(x)\right) - b_w \tau_t(x) \left(\frac{\mathrm{d}}{\mathrm{d}x} w_t(x)\right) \\ &\quad - b_w \sigma_{zzt}(x) - q_{zt} - N_{xxt}(x) \left(\frac{\mathrm{d}^2}{\mathrm{d}x^2} w_t(x)\right) - \frac{1}{2} b_w \left(\frac{\mathrm{d}}{\mathrm{d}x} \tau_t(x)\right) d_t - \left(\frac{\mathrm{d}}{\mathrm{d}x} N_{xxt}(x)\right) \left(\frac{\mathrm{d}}{\mathrm{d}x} w_t(x)\right) \\ &\quad - \frac{1}{2} b_w \left(\frac{\mathrm{d}}{\mathrm{d}x} \sigma_{zzt}(x)\right) \left(\frac{\partial}{\partial z_c} u_c(x, z_c)\right)\Big|_{z_c=0} d_t + \frac{1}{4} b_w \left(\frac{\mathrm{d}}{\mathrm{d}x} \tau_t(x)\right) d_t^2 \left(\frac{\mathrm{d}^2}{\mathrm{d}x^2} w_t(x)\right) \\ &\quad - \frac{1}{2} b_w \sigma_{zzt}(x) \left(\frac{\partial}{\partial x} \left(\left(\frac{\partial}{\partial z_c} u_c(x, z_c)\right)\Big|_{z_c=0}\right)\right) d_t = 0 \end{aligned} \tag{10}$$

$$-\frac{1}{2}b_w\tau_b(x)\left(\frac{\mathrm{d}^2}{\mathrm{d}x^2}w_b(x)\right)d_b+b_w\sigma_{zzb}(x)\left(\frac{\partial}{\partial z_c}u_c(x,z_c)\right)\Big|_{z_c=c_s(x)}+b_w\tau_b(x)\left(\frac{\mathrm{d}}{\mathrm{d}x}u_{ob}(x)\right)$$
$$-\left(\frac{\mathrm{d}}{\mathrm{d}x}N_{xxb}(x)\right)+b_w\tau_b(x)-n_{xb}=0 \tag{11}$$

$$\frac{1}{2}b_w\tau_b(x)d_b\left(\frac{\mathrm{d}^2}{\mathrm{d}x^2}u_{ob}(x)\right)-q_{zb}-\left(\frac{\mathrm{d}}{\mathrm{d}x}N_{xxb}(x)\right)\left(\frac{\mathrm{d}}{\mathrm{d}x}w_b(x)\right)-\left(\frac{\mathrm{d}^2}{\mathrm{d}x^2}M_{xxb}(x)\right)-\frac{1}{2}b_w\left(\frac{\mathrm{d}}{\mathrm{d}x}\tau_b(x)\right)d_b$$
$$+b_w\tau_b(x)\left(\frac{\mathrm{d}}{\mathrm{d}x}w_b(x)\right)+b_w\sigma_{zzb}(x)+b_w\sigma_{zzb}(x)\left(\frac{\partial}{\partial z_c}w_c(x,z_c)\right)\Big|_{z_c=c_s(x)}-\frac{1}{4}b_w\left(\frac{\mathrm{d}}{\mathrm{d}x}\tau_b(x)\right)d_b^2\left(\frac{\mathrm{d}^2}{\mathrm{d}x^2}w_b(x)\right)$$
$$+\left(\frac{\mathrm{d}}{\mathrm{d}x}m_b(x)\right)-\frac{1}{4}b_w\left(\frac{\mathrm{d}}{\mathrm{d}x}\tau_b(x)\right)d_b\left(\frac{\mathrm{d}}{\mathrm{d}x}u_{ob}(x)\right)-N_{xxb}(x)\left(\frac{\mathrm{d}^2}{\mathrm{d}x^2}w_b(x)\right)-\frac{1}{4}b_w\tau_b(x)d_b^2\left(\frac{\mathrm{d}^3}{\mathrm{d}x^3}w_b(x)\right)$$
$$-\frac{1}{2}b_w\left(\frac{\mathrm{d}}{\mathrm{d}x}\sigma_{zzb}(x)\right)\left(\frac{\partial}{\partial z_c}u_c(x,z_c)\right)\Big|_{z_c=c_s(x)}d_b-\frac{1}{2}b_w\sigma_{zzb}(x)d_b\left(\frac{\partial^2}{\partial x\partial z_c}u_c(x,z_c)\right)\Big|_{z_c=c_s(x)}$$
$$-\frac{1}{2}b_w\sigma_{zzb}(x)d_b\left(\frac{\partial^2}{\partial z_c^2}u_c(x,z_c)\right)\Big|_{z_c=c_s(x)}\left(\frac{\mathrm{d}}{\mathrm{d}x}c_s(x)\right)=0 \tag{12}$$

where, $\tau_j(x)$ and $\sigma_{zzj}(x)(j=t,b)$ are the shear and vertical normal stresses at the upper and the lower face–core interfaces, respectively.

The field equations for the core equal:

$$-b_w\left(\frac{\partial}{\partial x}\tau(x,z_c)\right)\left(\frac{\partial}{\partial z_c}u_c(x,z_c)\right)-2b_w\tau(x,z_c)\left(\frac{\partial^2}{\partial z_c\partial x}u_c(x,z_c)\right)-b_w\left(\frac{\partial}{\partial z_c}\tau(x,z_c)\right)$$
$$-b_w\left(\frac{\partial}{\partial z_c}\tau(x,z_c)\right)\left(\frac{\partial}{\partial x}u_c(x,z_c)\right)-b_w\left(\frac{\partial}{\partial z_c}\sigma_{zz}(x,z_c)\right)\left(\frac{\partial}{\partial z_c}u_c(x,z_c)\right)-b_w\sigma_{zz}(x,z_c)\left(\frac{\partial^2}{\partial z_c^2}u_c(x,z_c)\right)=0 \tag{13}$$

$$-b_w\left(\frac{\partial}{\partial x}\tau(x,z_c)\right)-b_w\left(\frac{\partial}{\partial x}\tau(x,z_c)\right)\left(\frac{\partial}{\partial z_c}w_c(x,z_c)\right)-2b_w\tau(x,z_c)\left(\frac{\partial^2}{\partial z_c\partial x}w_c(x,z_c)\right)$$
$$-b_w\left(\frac{\partial}{\partial z_c}\tau(x,z_c)\right)\left(\frac{\partial}{\partial x}w_c(x,z_c)\right)-b_w\left(\frac{\partial}{\partial z_c}\sigma_{zz}(x,z_c)\right)-b_w\left(\frac{\partial}{\partial z_c}\sigma_{zz}(x,z_c)\right)\left(\frac{\partial}{\partial z_c}w_c(x,z_c)\right)$$
$$-b_w\sigma_{zz}(x,z_c)\left(\frac{\partial^2}{\partial z_c^2}w_c(x,z_c)\right)$$
$$=0 \tag{14}$$

The solution of field equations starts first with an analytical/numerical solution of the core stress and displacements fields, and proceeds with the solution of the equations of the face sheets. Here, the field equations of the core appear as a set of very complicated non-linear partial differential equations with no known general analytical closed-form solution. Hence, a simplified approach must be used instead.

In the first approach, the kinematic relations of the shear angle of the core are kept non-linear and include the effect of the vertical core displacements only. The height of the core is modified to include the effects of the deformations of the upper and the lower face sheets. The distribution of the vertical normal stresses through the depth of the core is assumed to be linear, following the non-linear high-order sandwich panel approach (HSAPT).

In the second simplified approach, the non-linear kinematic relations of the core are replaced by the linear kinematic relations, and the upper limit of the integration through the depth of the core, see Eq. (2), is set equal to the height of the undeformed shape of the core, c, see Fig. 2e. This simplification yields the non-linear sandwich panel theory model (HSAPT), see Frostig and Baruch (1993).The quality of the simplified models is measured through the theoretical fulfillment of overall equilibrium in each of the models and comparison with FEA results obtained using ADINA, see Adina System (2003) and ANSYS, see Ansys ver. 7.1.

3. Simplified non-linear mathematical formulations

3.1. Non-linear core

The field equations for this case are based on the non-linear kinematic relations corresponding to moderate rotations, see Eqs. (4) and (5) (i.e. the von Karmann class of deformations), and take into account the deformed height of the core, see Fig. 2d, to be used in Eq. (2). The non-linear kinematic relations for the core are expressed through the shear angle only as follows:

$$\begin{aligned}\gamma_{xzc} &= u_{c,z_c}(x,z_c) + w_{c,x}(x,z_c) + w_{c,x}(x,z_c)w_{c,z_c}(x,z_c)\\ \varepsilon_{zzc} &= w_{c,z_c}(x,z_c)\end{aligned} \tag{15}$$

The field equations are derived using the non-linear kinematic relations of the face sheets, Eqs. (4) and (5), the non-linear kinematic relations of the core, Eq. (15), the compatibility conditions, Eq. (8), and the variations of the internal and the external energy, Eqs. (2) and (3). Hence, after integrations by parts and some algebraic manipulation they read:

For the upper and the lower face sheets:

$$-n_{xt} - \left(\frac{\mathrm{d}}{\mathrm{d}x}N_{xxt}(x)\right) - b_w\tau_t(x) = 0 \tag{16}$$

$$\begin{aligned}&\left(\frac{\mathrm{d}}{\mathrm{d}x}m_t(x)\right) - \left(\frac{\mathrm{d}}{\mathrm{d}x}N_{xxt}(x)\right)\left(\frac{\mathrm{d}}{\mathrm{d}x}w_t(x)\right) - N_{xxt}(x)\left(\frac{\mathrm{d}^2}{\mathrm{d}x^2}w_t(x)\right) - \left(\frac{\mathrm{d}^2}{\mathrm{d}x^2}M_{xxt}(x)\right) - q_t\\ &\quad - b_w\tau_t(x)\left(\frac{\mathrm{d}}{\mathrm{d}x}w_t(x)\right) - b_w\sigma_{zzt}(x) - \frac{1}{2}b_w\left(\frac{\mathrm{d}}{\mathrm{d}x}\tau_t(x)\right)d_t\\ &\quad = 0\end{aligned} \tag{17}$$

$$-\left(\frac{\mathrm{d}}{\mathrm{d}x}N_{xxb}(x)\right) - n_{xb} + b_w\tau_b(x) = 0 \tag{18}$$

$$\begin{aligned}&\left(\frac{\mathrm{d}}{\mathrm{d}x}m_b(x)\right) - q_b - \left(\frac{\mathrm{d}}{\mathrm{d}x}N_{xxb}(x)\right)\left(\frac{\mathrm{d}}{\mathrm{d}x}w_b(x)\right) - N_{xxb}(x)\left(\frac{\mathrm{d}^2}{\mathrm{d}x^2}w_b(x)\right) - \left(\frac{\mathrm{d}^2}{\mathrm{d}x^2}M_{xxb}(x)\right)\\ &\quad + b_w\tau_b(x)\left(\frac{\mathrm{d}}{\mathrm{d}x}w_b(x)\right) + b_w\sigma_{zzb}(x) - \frac{1}{2}b_w\left(\frac{\mathrm{d}}{\mathrm{d}x}\tau_b(x)\right)d_b\\ &\quad = 0\end{aligned} \tag{19}$$

For the core:

$$-b_w\left(\frac{\partial}{\partial z_c}\tau(x,z_c)\right) = 0 \tag{20}$$

$$
\begin{aligned}
&- b_w\left(\frac{\partial}{\partial x}\tau(x,z_c)\right) - b_w\left(\frac{\partial}{\partial x}\tau(x,z_c)\right)\left(\frac{\partial}{\partial z_c}w_c(x,z_c)\right) - 2b_w\tau(x,z_c)\left(\frac{\partial^2}{\partial z_c \partial x}w_c(x,z_c)\right)\\
&- b_w\left(\frac{\partial}{\partial z_c}\tau(x,z_c)\right)\left(\frac{\partial}{\partial x}w_c(x,z_c)\right) - \left(\frac{\partial}{\partial z_c}\sigma_{zz}(x,z_c)\right)b_w\\
&= 0
\end{aligned}
\tag{21}
$$

The first field equations of the core, Eq. (20), yields that the distribution of the shear stress through the depth of the core is uniform, similar to the case of the linear core, see second simplified model ahead. It reads:

$$\tau(x,z_c) = \tau_t(x) = \tau_b(x) = \tau(x) \tag{22}$$

The vertical displacement field of the core is determined from the second field equation of the core, see Eq. (21). However, since a closed-form analytical solution is impossible, an approximate solution is sought by assuming that the distribution of the vertical normal stresses is linear, as follows:

$$\sigma_{zz}(x,z_c) = \alpha(x)z_c + \sigma_{zzt}(x) \tag{23}$$

where $\alpha(x)$ is a function that has to be determined through the overall vertical equilibrium of the deformed core, see Fig. 2a, and $\sigma_{zzt}(x)$ is the vertical normal stress at the upper core–face interface.

The vertical equilibrium equation of the core considers as a whole reads:

$$
\begin{aligned}
&\sum F_z = \sigma_{zzb}(x) - \sigma_{zzt}(x) + \tau(x)\left(\frac{\mathrm{d}}{\mathrm{d}x}w_b(x)\right) - \tau(x)\left(\frac{\mathrm{d}}{\mathrm{d}x}w_t(x)\right) + \tau(x)\left(\frac{\mathrm{d}}{\mathrm{d}x}c_s(x)\right)\\
&+ \left(\frac{\mathrm{d}}{\mathrm{d}x}\tau(x)\right)c_s(x) + \left(\frac{\mathrm{d}}{\mathrm{d}x}\tau(x)\right)\left(\frac{\mathrm{d}}{\mathrm{d}x}c_s(x)\right)\\
&= 0
\end{aligned}
\tag{24}
$$

The unknowns $\alpha(x)$ and $\sigma_{zzt}(x)$ are determined through the solution of the distribution of the vertical displacement, the compatibility conditions in the vertical direction at the upper and the lower face sheets (see second equation in Eq. (8)) and the overall equilibrium in the vertical direction, Eq. (24). Hence, $\alpha(x)$ equals:

$$\alpha(x) = -\frac{2\tau(x)\left(\frac{\mathrm{d}}{\mathrm{d}x}c_s(x)\right) + \left(\frac{\mathrm{d}}{\mathrm{d}x}\tau(x)\right)c_s(x)}{c_s(x)} \tag{25}$$

The governing equations are derived through the use of linear constitutive relations (Hooke's law) for the face sheets and the core in the field equations, see Eqs. (16)–(19).

The field equations have been solved using the multiple points shooting method along with the parametric and arc-length continuation methods, see Stoer and Bulirsch (1980) and Keller (1992). The solution procedure uses the following set of governing first-order differential equations for the case of a panel with isotropic face sheets:

$$\frac{\mathrm{d}}{\mathrm{d}x}N_{xxt}(x) = -n_{xt} - b_w\tau(x) \tag{26}$$

$$\frac{\mathrm{d}}{\mathrm{d}x}u_{ot}(x) = \frac{N_{xxt}(x)}{EA_t(x)} - \frac{1}{2}Dw_t(x)^2 \tag{27}$$

$$\frac{\mathrm{d}}{\mathrm{d}x}V_{xzt}(x) = \frac{E_{zc}b_w w_t(x)}{c_s(x)} - Dw_t(x)\tau(x)b_w - \frac{E_{zc}b_w w_b(x)}{c_s(x)} - \left(\frac{\mathrm{d}}{\mathrm{d}x}c_s(x)\right)b_w\tau(x) - \frac{1}{2}E_{zc}\mathrm{Dtau}(x)c_s(x)b_w - q_{zt} \tag{28}$$

$$\frac{\mathrm{d}}{\mathrm{d}x}M_{xxt}(x) = -\frac{1}{2}b_w d_t\tau(x) + m_t(x) - N_{xxt}(x)Dw_t(x) + V_{xzt}(x) \tag{29}$$

$$\frac{\mathrm{d}}{\mathrm{d}x}w_t(x) = Dw_t(x) \tag{30}$$

$$\frac{\mathrm{d}}{\mathrm{d}x}Dw_t(x) = -\frac{M_{xxt}(x)}{EI_t(x)} \tag{31}$$

$$\frac{\mathrm{d}}{\mathrm{d}x}N_{xxb}(x) = -n_{xb} + b_w\tau(x) \tag{32}$$

$$\frac{\mathrm{d}}{\mathrm{d}x}u_{ob}(x) = \frac{N_{xxb}(x)}{EA_b(x)} - \frac{1}{2}Dw_b(x)^2 \tag{33}$$

$$\frac{\mathrm{d}}{\mathrm{d}x}V_{xzb}(x) = -\frac{E_{zc}b_w w_t(x)}{c_s(x)} + \frac{E_{zc}b_w w_b(x)}{c_s(x)} + b_w\tau(x)Dw_b(x) - \left(\frac{\mathrm{d}}{\mathrm{d}x}c_s(x)\right)b_w\tau(x) - \frac{1}{2}E_{zc}\mathrm{Dtau}(x)c_s(x)b_w - q_{zb} \tag{34}$$

$$\frac{\mathrm{d}}{\mathrm{d}x}M_{xxb}(x) = -N_{xxb}(x)Dw_b(x) - \frac{1}{2}b_w d_b\tau(x) + m_b(x) + V_{xzb}(x) \tag{35}$$

$$\frac{\mathrm{d}}{\mathrm{d}x}w_b(x) = Dw_b(x) \tag{36}$$

$$\frac{\mathrm{d}}{\mathrm{d}x}Dw_b(x) = -\frac{M_{xxb}(x)}{EI_b(x)} \tag{37}$$

$$\frac{\mathrm{d}}{\mathrm{d}x}\tau(x) = E_{zc}\mathrm{Dtau}(x) \tag{38}$$

$$\frac{\mathrm{d}}{\mathrm{d}x}\mathrm{Dtau}(x) = (\text{see Appendix A for details}) \tag{39}$$

where N_{xxj} and $M_{xxj}(j = t, b)$ are the in-plane stress and bending moment resultants of each face sheet; $V_{xzj}(j = t, b)$ are the shear stress resultants in the upper and lower face sheets; $\tau(x)$ is the shear stress in the core; w_j and $u_{oj}(j = t, b)$ are the vertical and mid-plane in-plane displacements of the face sheets; EA_j and EI_j are the in-plane and flexural rigidities of the face sheets; E_{zc} and G_{xzc} are the vertical modulus of elasticity and the shear modulus of the core; $b_w, d_j(j = t, b)$ and c are the width of the panel, the thickness of the upper and lower face sheets and the height of the core, respectively; x is the longitudinal coordinate of the sandwich panel. Reference is made to Fig. 2 for the adopted sign conventions and coordinates. It should be noted that the slope of the shear stress, see Eq. (38), has been scaled with respect to the modulus of elasticity of the core, E_{zc}, in order to achieve an efficient numerical scheme. Notice that the details of the lengthy compatibility equation, Eq. (39), appear in Appendix A, for simplicity and clarity.

The vertical normal stress field through the depth of the core reads:

$$\sigma_{zz}(x, z_c) = -\frac{\left(2\tau(x)\left(\frac{\mathrm{d}}{\mathrm{d}x}c_s(x)\right) + \left(\frac{\mathrm{d}}{\mathrm{d}x}\tau(x)\right)c_s(x)\right)z_c}{c_s(x)} - \frac{1}{2}\frac{-2c_s(x)\tau(x)\left(\frac{\mathrm{d}}{\mathrm{d}x}c_s(x)\right) - \left(\frac{\mathrm{d}}{\mathrm{d}x}\tau(x)\right)c_s(x)^2 + 2w_t(x)E_{zc} - 2w_b(x)E_{zc}}{c_s(x)} \tag{40}$$

and the vertical normal stresses at the upper and the lower face sheet equal:

$$\sigma_{zzt}(x) = \tau(x)\left(\frac{\mathrm{d}}{\mathrm{d}x}c_s(x)\right) + \frac{1}{2}\left(\frac{\mathrm{d}}{\mathrm{d}x}\tau(x)\right)c_s(x) - \frac{w_t(x)E_{zc}}{c_s(x)} + \frac{w_b(x)E_{zc}}{c_s(x)}$$
$$\sigma_{zzb}(x) = -\tau(x)\left(\frac{\mathrm{d}}{\mathrm{d}x}c_s(x)\right) - \frac{1}{2}\left(\frac{\mathrm{d}}{\mathrm{d}x}\tau(x)\right)c_s(x) - \frac{w_t(x)E_{zc}}{c_s(x)} + \frac{w_b(x)E_{zc}}{c_s(x)} \tag{41}$$

The vertical and the longitudinal displacements are derived using the non-linear kinematic relations of the core, see Eq. (15), and by the adoption of isotropic linear constitutive relations. Hence, the vertical displacement read:

$$w_c(x,z_c) = -\frac{1}{2}\frac{\left(2\tau(x)\left(\frac{\mathrm{d}}{\mathrm{d}x}c_s(x)\right) + \left(\frac{\mathrm{d}}{\mathrm{d}x}\tau(x)\right)c_s(x)\right)z_c^2}{E_{zc}c_s(x)} + \frac{1}{2}\frac{\left(2c_s(x)\tau(x)\left(\frac{\mathrm{d}}{\mathrm{d}x}c_s(x)\right) + \left(\frac{\mathrm{d}}{\mathrm{d}x}\tau(x)\right)c_s(x)^2 - 2w_t(x)E_{zc} + 2w_b(x)E_{zc}\right)z_c}{E_{zc}c_s(x)} + w_t(x) \tag{42}$$

The distribution of the longitudinal displacement in the core has been derived analytically using linear constitutive relations of an isotropic core, and the kinematic relations that appear in the first equation of Eq. (15). The expression of the longitudinal displacement is complex and very lengthy, and for brevity it is omitted. The explicit expression for the in-plane core displacement, however, has been used to derive Eq. (39), which is equivalent to the compatibility condition at the lower face–core interface in the longitudinal direction, see the first equation in Eq. (8). Please notice that, in this case, the stress field in the core fulfills equilibrium in the overall sense and not in the differential sense, i.e. Eq. (21) is not fulfilled.

In order to verify the quality of the solution the overall equilibrium equations of a deformed differential segment are derived analytically. First, the overall in-plane and shear stress resultants as well as the bending moment resultants are defined using the stress resultants in the face sheets and the core, see Fig. 2c and d. They read:

$$N_G(x) = N_{xxt}(x) + N_{xxb}(x) \tag{43}$$

$$M_G(x) = M_{xxt}(x) + M_{xxb}(x) - N_{xxt}(x)\left(c + \frac{1}{2}d_t + \frac{1}{2}d_b + w_b(x) - w_t(x)\right) \tag{44}$$

$$V_G(x) = V_{xzt}(x) + V_{xzb}(x) + V_{xzc}(x) \tag{45}$$

where $V_{xzc} = \tau(x)b_w c$, and the subscript G refers to the term "global".

The overall equilibrium equations are derived using the governing equations, Eqs. (26)–(39). The overall equilibrium equation of the summation of forces in the longitudinal directions equals the sum of Eqs. (26) and (32), and that of equilibrium in the vertical direction consist of the sum of Eqs. (28) and (34) and the derivative of V_{xzc}. The overall moment equilibrium equation equals the sum of Eqs. (26), (29) and (35) and some algebraic manipulations. Hence, the overall equilibrium equations, assuming $n_{xt} = 0$ and $n_{xb} = 0$ equal:

$$\frac{\mathrm{d}}{\mathrm{d}x}N_G(x) = 0 \tag{46}$$

$$\frac{\mathrm{d}}{\mathrm{d}x}V_G(x) = -q_{zt} - q_{zb} \tag{47}$$

$$\frac{\mathrm{d}}{\mathrm{d}x}M_G(x) = V_G(x) + m_t(x) + m_b(x) \tag{48}$$

All the three equations are in accordance with the overall equilibrium requirements, see Fig. 2c. Accordingly, this simplified model fulfills accurately the conditions of overall equilibrium in the full range of large deformations with moderate rotations.

3.2. Linear core

In the second simplified model it is assumed that the face sheets undergo large deformations with moderate rotations, i.e. the so called "intermediate" class of deformations, whereas the kinematic relations of the core are assumed to be linear and equal to those corresponding to small deformations and small rotations. It means that the face sheets are deformed, while the core is considered in its undeformed state, see Fig. 2e. This approach coincides with the Non-Linear High-Order Sandwich Panel (NLHSAPT) approach, and the set of the non-linear governing equations used for this analysis appears in Frostig and Baruch (1993). Here, the upper limit of the integration of the core, see Eq. (2), changes into c and the kinematic relation of the core read:

$$\begin{aligned}\gamma_{xzc} &= u_{c,z_c}(x,z_c) + w_{c,x}(x,z_c)\\ \varepsilon_{zzc} &= w_{c,z_c}(x,z_c)\end{aligned} \tag{49}$$

The field equations, for this case, have been derived in a similar way to that of the previous case. The equilibrium equations in the longitudinal direction at the upper and the lower face sheet are identical, see Eqs. (16) and (18). However, the equations of the equilibrium in the vertical directions of the upper and the lower face sheets are different, see Eqs. (17) and (19), and they read:

$$\begin{aligned}&-N_{xxt}(x)\left(\frac{\mathrm{d}^2}{\mathrm{d}x^2}w_t(x)\right) - \left(\frac{\mathrm{d}}{\mathrm{d}x}N_{xxt}(x)\right)\left(\frac{\mathrm{d}}{\mathrm{d}x}w_t(x)\right) - \left(\frac{\mathrm{d}^2}{\mathrm{d}x^2}M_{xxt}(x)\right) - q_t + \left(\frac{\mathrm{d}}{\mathrm{d}x}m_t(x)\right) - b_w\sigma_{zzt}(x)\\ &\quad - \frac{1}{2}b_w d_t\left(\frac{\mathrm{d}}{\mathrm{d}x}\tau_t(x)\right)\\ &\quad = 0\end{aligned} \tag{50}$$

$$\begin{aligned}&-q_b - Nxx_b(x)\left(\frac{\mathrm{d}^2}{\mathrm{d}x^2}w_b(x)\right) - \left(\frac{\mathrm{d}}{\mathrm{d}x}Nxx_b(x)\right)\left(\frac{\mathrm{d}}{\mathrm{d}x}w_b(x)\right) - \left(\frac{\mathrm{d}^2}{\mathrm{d}x^2}Mxx_b(x)\right) + \left(\frac{\mathrm{d}}{\mathrm{d}x}m_b(x)\right)\\ &\quad + b_w\sigma_{zzb}(x) - \frac{1}{2}b_w d_b\left(\frac{\mathrm{d}}{\mathrm{d}x}\tau_b(x)\right)\\ &\quad = 0\end{aligned} \tag{51}$$

The equilibrium equations for the core are also partly different from those of the previous case. The core in-plane equilibrium equations for the two cases, see Eq. (20), are identical, while the equation of vertical equilibrium, see Eq. (21), is different and reads:

$$-\left(\frac{\partial}{\partial x}\tau(x,z_c)\right)b_w - \left(\frac{\partial}{\partial z_c}\sigma_{zz}(x,z_c)\right)b_w = 0 \tag{52}$$

The solution of the field equations of the core yields that the distribution of the shear stresses through the depth of the core is uniform as in the previous case, see Eq. (22). In addition, the distribution of the vertical normal stresses is linear, similar to Eq. (23) but with different coefficients. It should be noticed that here the stress field satisfies the conditions of equilibrium in the differential sense as well as in the overall sense, which is in contrast with the previous case.

The set of governing equations are almost identical with those obtained for the case of a non-linear deformed core (previous case), but with some differences in the following equations. The shear force equations for the upper and the lower face sheets are different, see Eqs. (28) and (34) and they read:

$$\frac{\mathrm{d}}{\mathrm{d}x}V_{xzt}(x) = -\frac{b_w E_{zc} w_b(x)}{c} + \frac{b_w E_{zc} w_t(x)}{c} - \frac{1}{2}E_{zc}\mathrm{Dtau}(x) b_w c - q_{zt} \tag{53}$$

$$\frac{\mathrm{d}}{\mathrm{d}x}V_{xzb}(x) = \frac{b_w E_{zc} w_b(x)}{c} - \frac{b_w E_{zc} w_t(x)}{c} - \frac{1}{2}E_{zc}\mathrm{Dtau}(x) b_w c - q_{zb} \tag{54}$$

The compatibility equation for the undeformed core is much simpler then that of the previous case (see Eq. (39) for the model with the non-linear core):

$$\frac{\mathrm{d}}{\mathrm{d}x}\mathrm{Dtau}(x) = -\frac{12\left(-u_{ot}(x) + u_{ob}(x) + \frac{1}{2}(c + d_t)Dw_t(x) + \frac{1}{2}(c + d_b)Dw_b(x) - \frac{c\tau(x)}{G_{xzc}}\right)}{c^3} \tag{55}$$

The stress and the deformation fields in for the case of an undeformed core have been solved analytically assuming an isotropic core with linear constitutive relations, and they read:

$$\sigma_{zz}(x, z_c) = \left(\frac{c}{2} - z_c\right)E_{zc}\mathrm{Dtau}(x) + \frac{(w_b(x) - w_t(x))E_{zc}}{c} \tag{56}$$

$$\sigma_{zzt}(x) = \frac{(w_b(x) - w_t(x))E_{zc}}{c} + \frac{1}{2}cE_{zc}\mathrm{Dtau}(x) \tag{57}$$

$$\sigma_{zzb}(x) = \frac{(w_b(x) - w_t(x))E_{zc}}{c} - \frac{1}{2}cE_{zc}\mathrm{Dtau}(x) \tag{58}$$

$$w_c(x, z_c) = \left(\frac{1}{2}cz_c - \frac{1}{2}z_c^2\right)\mathrm{Dtau}(x) + \left(1 - \frac{z_c}{c}\right)w_t(x) + \frac{z_c w_b(x)}{c} \tag{59}$$

$$u_c(x, z_c) = \frac{z_c\tau(x)}{G_{xzc}} + \left(-\frac{1}{4}cz_c^2 + \frac{1}{6}z_c^3\right)\left(\frac{\mathrm{d}}{\mathrm{d}x}\mathrm{Dtau}(x)\right) + u_{ot}(x) + \left(-z_c + \frac{1}{2}\frac{z_c^2}{c} - \frac{1}{2}d_t\right)Dw_t(x) - \frac{1}{2}\frac{z_c^2 Dw_b(x)}{c} \tag{60}$$

where $\sigma_{zz}(x, z_c)$ are the distribution of the transverse normal stresses of the core; $\sigma_{zzj}(x)(j = t, b)$ are the transverse (vertical) normal stresses at the upper and the lower face–core interfaces. Reference is made to Fig. 2 for sign conventions. The full derivation of Eqs. (49)–(60) can be found in Frostig and Baruch (1993).

The overall equilibrium equations at any section of the sandwich panel are derived following the procedure that is described in the previous case, see Eqs. (36)–(41). Using the same overall stress resultant, see Eqs. (43)–(45), yields the same overall equilibrium equations for the longitudinal directions, see Eq. (46), and the for the vertical directions, see Eq. (47). The bending equilibrium equation is different than that of the previous case with the deformed core, and it equals:

$$\frac{\mathrm{d}}{\mathrm{d}x}M_G(x) = b_w\tau(x)w_b(x) - b_w\tau(x)w_t(x) + m_t(x) + V_G(x) + m_b(x) \tag{61}$$

This equation, see Fig. 2c, does not fulfill the overall condition of moment equilibrium, and it includes additional terms due to the shear stresses at the upper and the lower interfaces between the core and the face sheets. This discrepancy is small when the difference between the vertical displacements of the upper and the lower face sheets is small, and it is null when the vertical displacements are identical. Usually, as along as the core does not undergo large indentations, i.e. $w_t(x) \gg w_b(x)$, the discrepancy in Eq. (61) is small or in other words, the overall equilibrium is retained with good approximation in spite of the theoretical discrepancy. Please notice, that in the previous case this equation is accurately fulfilled. It means

that from an analytical point of view the simplification with the non-linear core is better then the model with the linear one. How this discrepancy affects the predicted behavior, and how good the simplified models when compared with numerical FEA results are, is presented next.

4. Three point bending—numerical example

The objective of presenting the numerical example of a sandwich panel loaded in three-point bending is to investigate the accuracy of the simplified models as compared with a numerical FEA results obtained with ADINA, ver. 8.1 (Adina System, 2003) and Ansys ver. 7.1. The sandwich panel consists of two face sheets made of Kevlar with an equivalent modulus of elasticity of 27.4 GPa and a lightweight, low strength core of Rohacell 50 with $E_{zc} = 52.5\,\text{MPa}$ and $G_{xzc} = 21.0\,\text{MPa}$. The geometry of the panel appears in Fig. 3a.

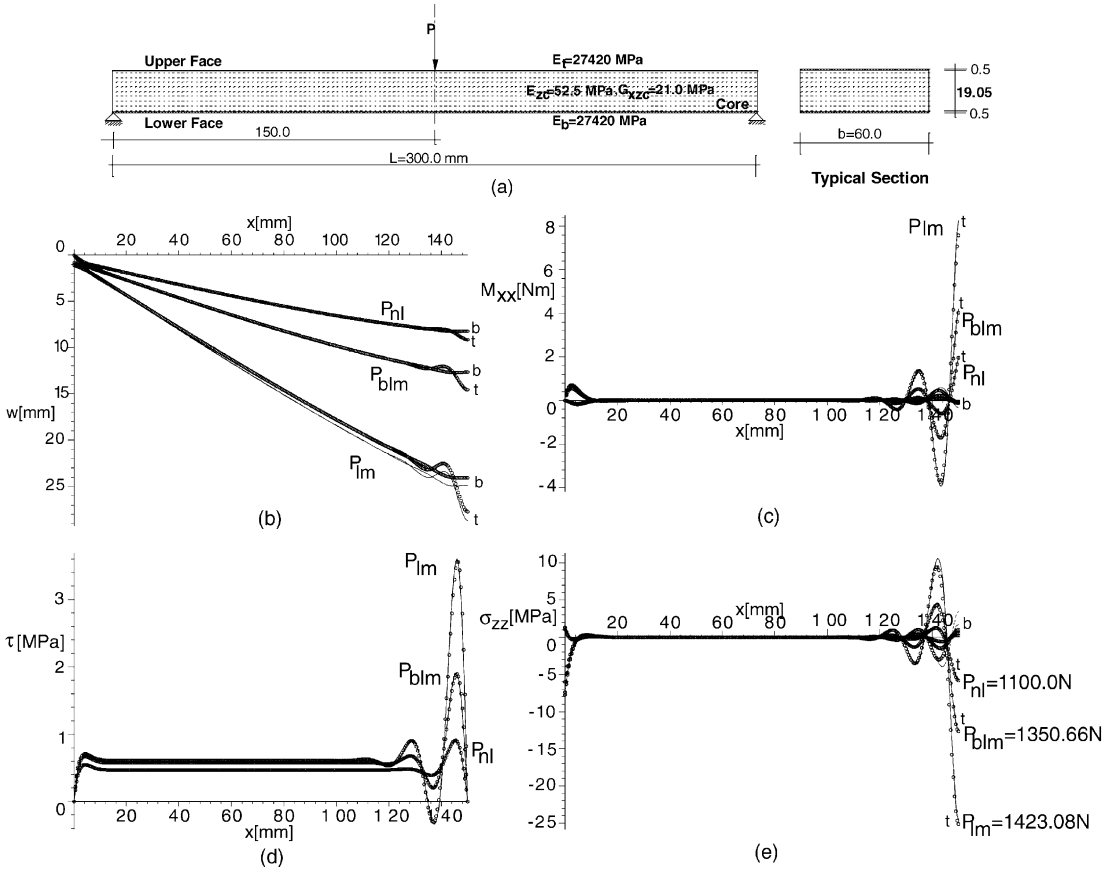

Fig. 3. Geometry and results of models in face sheets and core–face interfaces along half length of panel at various load levels: (a) geometry, (b) vertical displacements, (c) bending moments of face sheets, (d) shear stresses in core, (e) interfacial vertical normal stresses at core–face interfaces. Legend: __t upper face/interface, --- b Lower face/interface, ○○○ Model with Deformed core (DefC).

The numerical solutions of the simplified models have been achieved using the multiple-shooting point method along with a parametric and an arc-length continuation procedure to reveal possible limit-point behavior. The solution procedures only consider half of the panel length due to the symmetry at mid-span.

The results in the form of displacements, bending moments, core shear stresses and vertical normal stresses at the face–core interfaces along the half length of the panel corresponding to the two simplified formulations are presented at different load levels. Firstly, at a load level in the linear state, with $P_{nl} = 1.1\,\mathrm{kN}$. Secondly deep into the non-linear regime, at a load level below the limit point, with $P_{blm} = 1.351\,\mathrm{kN}$, with a deflection that equals that of the limit point due to ADINA. Thirdly, at the limit point, $P_{lm} = 1.423\,\mathrm{kN}$. The results are displayed in Fig. 3. The results of the two simplified model are almost identical in both the linear and non-linear regimes. At the limit point load level some differences between the two models are observed, but they are small. The overall equilibrium requirements, in accordance with Eqs. (43)–(45), have been used to quantify the accuracy and quality of the two models. In the simplified model with the deformed core, all three equilibrium requirements have been accurately fulfilled, at all load levels, while in the case of the undeformed core the axial and shear force conditions have been accurately been fulfilled at all load levels, while the overall bending moment condition is fully fulfilled only at load levels below the limit point load. At the limit point there is a discrepancy in the overall bending moment but it is rather small.

The FEA model and its deformed shape using ADINA, see Adina System (2003), appears in Fig. 4. The modeling is based on the assumption of an isotropic core with $E_{zc} = E_{xc} = 52.5\,\mathrm{MPa}$ and $G_{xzc} = 21.0\,\mathrm{MPa}$ with the option of large deformations and large rotations. The limit point load of the ADINA run equals 1415.5 N. In the Ansys run an orthotropic core has been used with $E_{zc} = 52.5\,\mathrm{MPa}$, $E_{xc} = E_{zc}/10$ and $G_{xzc} = 21.0\,\mathrm{MPa}$ with the option of large deformations and large rotations. The limit point in this case is 1370.4 N.

The FEA analyses include models prepared in ADINA and in ANSYS, ver. 7.1. The ANSYS code has been used due to its widespread applications in the sandwich structures industry. The FEA models consist of a sandwich panel with an isotropic or orthotropic core, where its longitudinal rigidity is considered or reduced and with the large deformation option. Half and full length panels have been considered with identical results. The ratio of 1/500 between the modulus of elasticity of the core to that of the face sheets lead to numerical difficulties in ANSYS and ADINA. The low modulus of elasticity of the core causes large distortions in the core elements, which are beyond the numerical capabilities of ordinary elements and here has required the use of special elements with special options.

The ANSYS model uses solid elements for the face sheets and the core, with 8 nodes or a 4 node special element (solid plane 82). The eight nodes element stiffens the panel and fails to detect the limit point

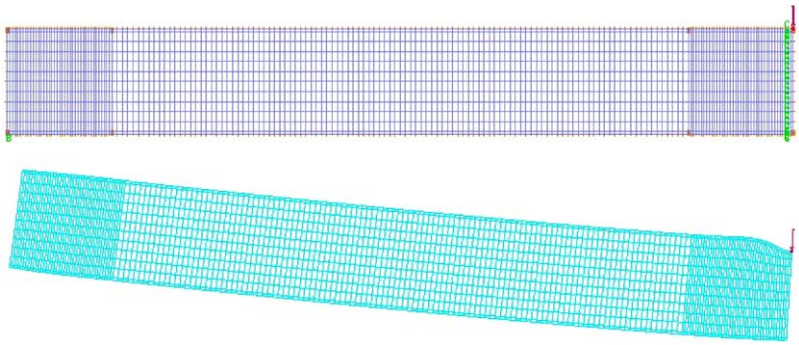

Fig. 4. Finite element model and its deformed shape due to Adina.

behavior, while the special element with four nodes has succeed to detect the limit point behavior but only for an orthotropic core where its modulus of elasticity in the longitudinal direction is assumed to be a tenth of that in the vertical direction. The value of the load at the limit point is about 1370.4 N. The model with four nodes consists of a very fine mesh that includes 8 elements through the thickness of each face sheet, and 19 elements through the thickness of the core. The analysis suffered from numerical instabilities and poor convergence caused by the large distortions in the elements of the core.

The ADINA model consists of a very fine mesh with 2D elements of nine nodes for the core and the face sheets, see Fig. 4a. This FEA model has detected the limit point behavior for the isotropic and orthotropic core, but with numerical difficulties caused by the large distortions of the elements of the core, which in some runs causes penetration of the loaded face sheet into the core.

Hence, the two FEA runs, for this particular case of a sandwich panel with a ''soft'' core, are associated with numerical difficulties that require a very experienced user with a large background and experience with non-linear FEA modeling.

The load versus the vertical displacement at the mid-span appears in Fig. 5. The results include the vertical displacements at the lower face sheets of the two simplified models that are cut off at 1/10th of the beam span, and the vertical displacement of the upper face sheet as obtained from the FEA runs. The load–displacement curve of the simplified models exhibits limit point behavior at a load level of 1423 N when the displacement is extended to beyond 1/10th of the beam span. The results of the two simplified models almost coincide through the entire range of results, even deep into the non-linear regime. The FEA results of ANSYS and ADINA, and those of the simplified models, are nearly identical through the entire range, except in the vicinity of the limit point. The displacements in the simplified models are larger than those of the FEA results, but with almost the same limit point load level. In the simplified models, the limit point load level equals 1423 N, while prediction of ADINA is 1415.5 N and that by ANSYS is 1370.4 N. Thus the limit point loads predicted by the simplified models and the FEA simulations are almost identical, while the displacements of the simplified models are much larger than those of the FEA, see Fig. 5. This discrepancy in the displacements is a result of the very low rigidity of the sandwich panel in the vicinity of the limit point. The behavior of the sandwich panel in the vicinity of the limit point load is attributed to the buckling of the upper compressed face sheet, and to the loss of the composite action of the sandwich panel, i.e the inability to increase the compressive and tensile forces in the upper and the lower face sheets and the shear stresses in the core. Hence, the result is a sandwich panel with a very

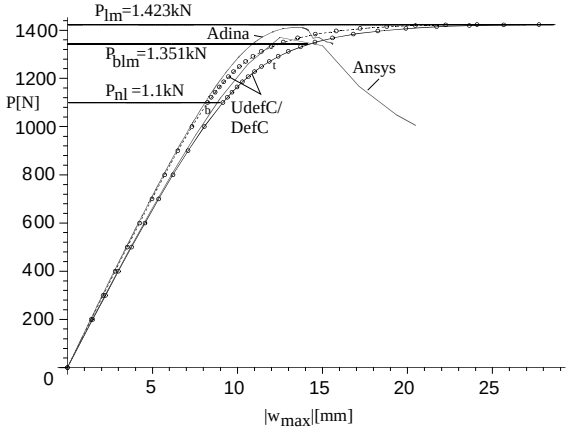

Fig. 5. Load versus mid-span displacement of simplified models and Adina. Legend: __t upper face, --- b Lower face, ○○○ Model with Deformed core (DefC).

low bending resistance that yields large bending moments and large deformations in the face sheets and in the panel as a whole for very small changes in the external load. The external load, at this stage, is resisted, mainly, through the bending resistance of each of the faces independently. Part of the load is transferred to the lower face sheet, mainly through vertical normal stresses in the core in the vicinity of the load, which leads to very large displacements. Please notice that, in the vicinity of the limit point, the displacements pattern of the two face sheets is almost identical.

A comparison between the two simplified models of the load versus the bending moments, the axial stress resultants in the face sheets, the shear stresses in the core and the interfacial vertical normal stresses at the upper and the lower face–core interfaces appears in Fig. 6. The results reveal that the two simplified models yield almost identical results with minor discrepancies.

The stress and displacements distributions in the core material at the support and at mid-span reveal some differences between the two models, see Fig. 7. Notice that the results for the case with the deformed core are drawn on the deformed height of the core. The results are described at the previously mentioned load levels, see Figs. 3 and 5. The distributions at the left support include the vertical normal stresses, the vertical and the longitudinal displacements. The largest discrepancy occurs at the limit point load level in the longitudinal displacement plot. At mid-span, see Fig. 7a_2 and b_2, the discrepancies between the two models is significant for the vertical normal stresses at the limit point load level. Here, the vertical interfacial stresses, in the case of the undeformed core, are in tension at the lower face–core interface, while they are almost zero in the other cases. In all other case, when the load is smaller than the limit point load level, the two approaches yield almost identical results with very small discrepancies.

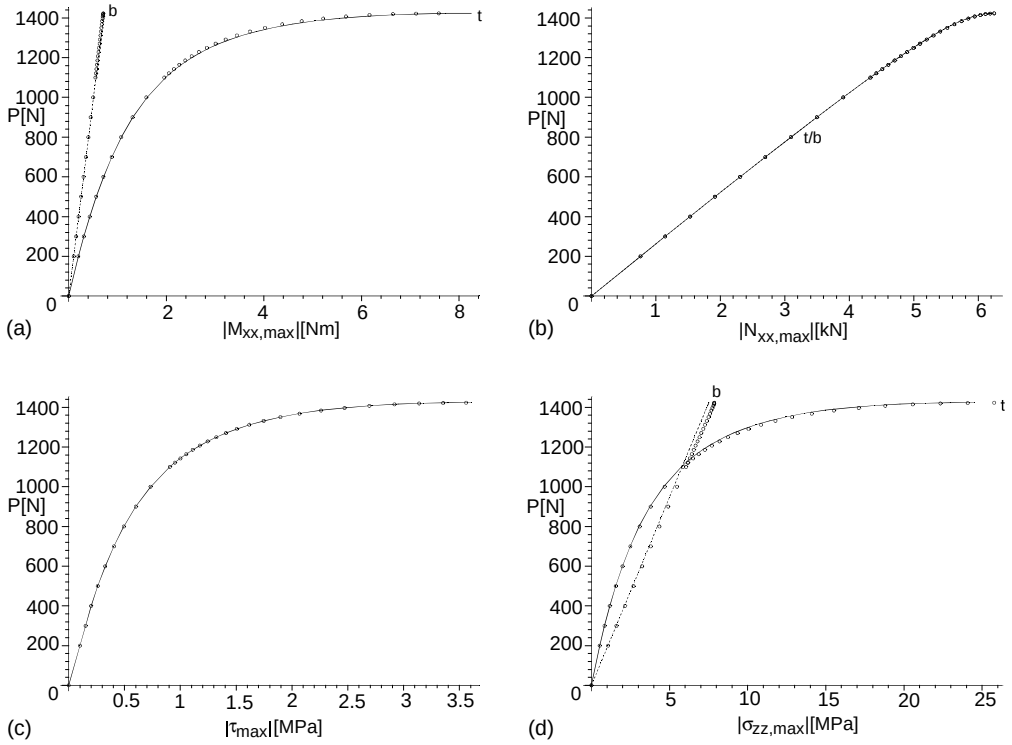

Fig. 6. Non-linear response curves, load versus extreme absolute structural quantities, of the simplified models: (a) bending moments and (b) inplane forces in faces, (c) shear stress in core, (d) interfacial vertical normal stresses at face–core interfaces. Legend: __t upper face/interface, --- b Lower face/interface, ○○○ Model with Deformed core.

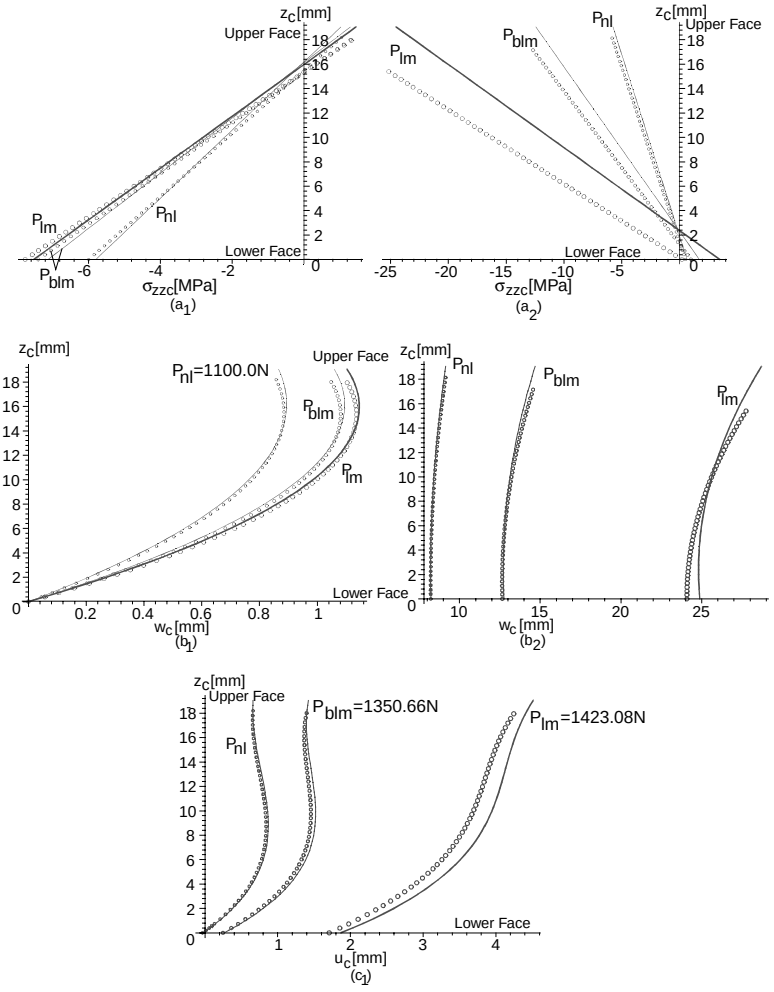

Fig. 7. Stress and displacement distributions in core material above support and at mid-span in models at three load levels: (a) vertical normal stresses, (b) vertical displacement, (3) longitudinal displacement. Legend: _ Model with Undeformed Core, ○○○ Model with Deformed core (curves on deformed height of core), 1—at support, 2—at mid-span.

5. Summary and conclusions

The governing equations of a sandwich panel, which has a transversely flexible core with negligible flexural rigidity, including large displacements and moderate rotations in the face sheets and the core, are presented using a variational approach. In this approach the sandwich model is described through two face sheets with in-plane and flexural rigidities, whereas the core is considered as a 2D elastic continuum that undergoes large displacements with moderate rotations. The formulation takes into account that the core is located between two face sheets that undergo large displacements, which change the height of the core and affects the volume of the core. This phenomenon is included in the variational formulation through the definition of the limits of the volume integral of the core. The resulting governing equations of the core are rather complex, and the stress and displacements fields in the core are described through a set of nonlinear partial differential equations without a general analytical solution.

Two simplified models have been adopted due to their ability to analytically describe the stress and the deformations fields in the core. The first model takes into account the deformed core and uses simplified non-linear kinematic relations while and the other one assumes that the core is undeformed and its kinematic relations are linear. Their accuracy is measured through the theoretical fulfillment of the overall equilibrium at any section throughout the length of the panel. The two models have been solved using the multiple points shooting method along with the parametric and the arc-length method. At all load levels, the two models yield almost identical results and the largest discrepancy occurs only in the vicinity of the limit point load level. However, the computer time required for the solution of model with the deformed core is ten times that of the undeformed core.

The models have been verified through comparison with FEA results expressed in terms of load versus mid-span displacement of the loaded face sheet of a sandwich panel loaded in a three point bending scheme. The ADINA FEA model consists of an isotropic core while the ANSYS model included a reduced modulus of elasticity in the longitudinal direction. The FEA runs are associated with numerical difficulties and poor convergence as a result of the large distortions that the finite elements of the core undergo in the vicinity of the limit point. The limit point loads obtained for all four cases are almost identical and very close to each other, while the displacements of the simplified models are much larger then those of the FEA ones. The curves of loads versus displacement of the simplified models are very similar to those of the FEA runs up to the limit point load. In the vicinity of the limit point load the simplified models exhibit larger displacement as a result of the null flexural rigidity of the core. It is important to notice that, at the limit point load level, the sandwich panel looses its composite action, as a result of the buckling of the compressed face sheet, and its flexural resistance drops to that of the isolated face sheets in the case of the simplified models, and to that of the isolated face sheets and the isolated core in the case of the FEA models. At this stage, in the simplified model, the core behaves more as a Winkler type of elastic foundation, in the vicinity of the load, which distributes the external load between the two face sheets. In the case of an isotropic or orthotropic core used in the FEA models, the deformations in the vicinity of the limit point are smaller as compared with those with a core that has no flexural rigidity.

The comparison between the simplified models and the FEA models reveals that the simplified model, with the undeformed core, is accurate through the entire loading range up to the limit point load level, and that it detects the limit point load correctly. The flexural rigidity of the core contributes to the resistance of the structure only when loss of the composite action occurs. Thus, in the vicinity of the limit point load level, the displacements of the simplified model are larger then those obtained with the FEA models. The simplified model is not associated with numerical instabilities and detects the limit point load flawlessly. Therefore, the use of a simplified model of the high-order theory assuming an undeformed core is more than justified in the analyses of sandwich panels with a "soft" core even when the sandwich panel undergoes large displacements with moderate rotations.

Acknowledgments

The ANSYS runs have been conducted by Mrs. Hilla Schwarts-Givli. Her assistance is gratefully acknowledged.

The work presented was conducted during the period of a visiting professorship of the first author with the Institute of Mechanical Engineering at Aalborg University in September 2003. The visiting professorship and the research presented herein were sponsored by the Danish Research Agency under the overall program on "Materials Research" within the framework of the specific research program "Novel Principles for Analysis and Design of Advanced Lightweight Composite and Sandwich Structures". The financial support received is gratefully acknowledged.

Appendix A. Compatibility equation of first simplified approach—non-linear core

$$
\begin{aligned}
\frac{\mathrm{d}}{\mathrm{d}x}\mathrm{Dtau}(x) = {} & \frac{12u_{ot}(x)}{c_s(x)^2(w_b(x)-w_t(x)+c_s(x))} - \frac{12u_{ob}(x)}{c_s(x)^2(w_b(x)-w_t(x)+c_s(x))} \\
& + \left(-\frac{\mathrm{Dtau}(x)}{w_b(x)-w_t(x)+c_s(x)} - \frac{2\left(\frac{\mathrm{d}}{\mathrm{d}x}c_s(x)\right)\tau(x)}{c_s(x)E_{zc}(w_b(x)-w_t(x)+c_s(x))} \right. \\
& \left. + \frac{1}{2}\left(-12c_s(x)^2E_{zc}^2G_{xzc} - 12d_tc_s(x)E_{zc}^2G_{xzc} + 12w_t(x)c_s(x)E_{zc}^2G_{xzc} - 12w_b(x)c_s(x)E_{zc}^2G_{xzc}\right) \right. \\
& \left. \Big/ \left(c_s(x)^3E_{zc}^2G_{xzc}(w_b(x)-w_t(x)+c_s(x))\right) \right) Dw_t(x) \\
& + \left(\frac{\mathrm{Dtau}(x)}{w_b(x)-w_t(x)+c_s(x)} + \frac{2\left(\frac{\mathrm{d}}{\mathrm{d}x}c_s(x)\right)\tau(x)}{c_s(x)E_{zc}(w_b(x)-w_t(x)+c_s(x))} \right. \\
& + \frac{1}{2}\left(-12c_s(x)^2E_{zc}^2G_{xzc} - 12w_b(x)c_s(x)E_{zc}^2G_{xzc} - 12d_bc_s(x)E_{zc}^2G_{xzc} \right. \\
& \left. \left. +12w_t(x)c_s(x)E_{zc}^2G_{xzc} \right) \Big/ \left(c_s(x)^3E_{zc}^2G_{xzc}(w_b(x)-w_t(x)+c_s(x))\right) \right) Dw_b(x) \\
& + \frac{1}{2}\frac{c_s(x)\left(\frac{\mathrm{d}}{\mathrm{d}x}c_s(x)\right)\mathrm{Dtau}(x)^2}{w_b(x)-w_t(x)+c_s(x)} + \left(\frac{2\left(\frac{\mathrm{d}}{\mathrm{d}x}c_s(x)\right)^2\tau(x)}{E_{zc}(w_b(x)-w_t(x)+c_s(x))} \right. \\
& + \frac{1}{2}\left(-10c_s(x)^3\left(\frac{\mathrm{d}}{\mathrm{d}x}c_s(x)\right)E_{zc}^2G_{xzc} + 12w_t(x)c_s(x)^2\left(\frac{\mathrm{d}}{\mathrm{d}x}c_s(x)\right)E_{zc}^2G_{xzc} \right. \\
& \left. \left. -12w_b(x)c_s(x)^2\left(\frac{\mathrm{d}}{\mathrm{d}x}c_s(x)\right)E_{zc}^2G_{xzc} \right) \Big/ \left(c_s(x)^3E_{zc}^2G_{xzc}(w_b(x)-w_t(x)+c_s(x))\right) \right) \mathrm{Dtau}(x) \\
& + \frac{2\left(\frac{\mathrm{d}}{\mathrm{d}x}c_s(x)\right)^3\tau(x)^2}{c_s(x)E_{zc}^2(w_b(x)-w_t(x)+c_s(x))} + \frac{1}{2}\left(-4w_b(x)c_s(x)^2\left(\frac{\mathrm{d}^2}{\mathrm{d}x^2}c_s(x)\right)E_{zc}G_{xzc} \right. \\
& + 4w_t(x)c_s(x)^2\left(\frac{\mathrm{d}^2}{\mathrm{d}x^2}c_s(x)\right)E_{zc}G_{xzc} + 24c_s(x)^2E_{zc}^2 + 12w_t(x)\left(\frac{\mathrm{d}}{\mathrm{d}x}c_s(x)\right)^2c_s(x)E_{zc}G_{xzc} \\
& - 8c_s(x)^2\left(\frac{\mathrm{d}}{\mathrm{d}x}c_s(x)\right)^2E_{zc}G_{xzc} - 4c_s(x)^3\left(\frac{\mathrm{d}^2}{\mathrm{d}x^2}c_s(x)\right)E_{zc}G_{xzc} \\
& \left. -12w_b(x)\left(\frac{\mathrm{d}}{\mathrm{d}x}c_s(x)\right)^2c_s(x)E_{zc}G_{xzc} \right) \tau(x) \Big/ \left(c_s(x)^3E_{zc}^2G_{xzc}(w_b(x)-w_t(x)+c_s(x))\right) \\
& + \frac{1}{2}\left(12\left(\frac{\mathrm{d}}{\mathrm{d}x}c_s(x)\right)w_b(x)^2E_{zc}^2G_{xzc} + 12w_b(x)\left(\frac{\mathrm{d}}{\mathrm{d}x}c_s(x)\right)c_s(x)E_{zc}^2G_{xzc} \right. \\
& - 12w_t(x)\left(\frac{\mathrm{d}}{\mathrm{d}x}c_s(x)\right)c_s(x)E_{zc}^2G_{xzc} - 24w_t(x)w_b(x)\left(\frac{\mathrm{d}}{\mathrm{d}x}c_s(x)\right)E_{zc}^2G_{xzc} \\
& \left. +12\left(\frac{\mathrm{d}}{\mathrm{d}x}c_s(x)\right)w_t(x)^2E_{zc}^2G_{xzc} \right) \Big/ \left(c_s(x)^3E_{zc}^2G_{xzc}(w_b(x)-w_t(x)+c_s(x))\right)
\end{aligned}
$$

References

Adina System 8.1. June 2003, Adina R&D, MA, USA.

Allen, H.G., 1969. Analysis and Design of Structural Sandwich Panels. London, Pergamon Press.

Ansys ver. 7.1. Swanson Analysis Systems, Inc., Houston, PA.

Frostig, Y., 1992. Behavior of delaminated sandwich beams with transversely flexible core high order theory. Composite Structures Journal 20, 1–16.

Frostig, Y., 1998. Buckling of sandwich panels with a transversely flexible core—high-order theory. International Journal of Solids and Structures 35 (3–4), 183–204.

Frostig, Y., Baruch, M., 1993. Buckling of simply-supported sandwich beams with transversely flexible core—a high order theory. Journal of. ASCE, EM Division 119 (3), 476–495.

Frostig, Y., Baruch, M., Vilnay, O., Sheinman, I., 1992. A high order theory for the bending of sandwich beams with a flexible core. Journal off ASCE, EM Division 118 (5), 1026–1043.

Hohe, J., Librescu, L., 2003. A nonlinear theory for doubly curved anisotropic sandwich shells with transversely compressible core. International Journal of Solids and Structures 40 (5), 1059–1088.

Huang, H.Y., Kardomateas, G.A., 2002. Buckling and initial postbuckling behavior of sandwich beams including transverse shear. AIAA Journal 40 (11), 2331–2335.

Kardomateas, G.A., Huang, H., 2003. The initial post-buckling behavior of face-sheet delaminations in sandwich composites. Journal of Applied Mechanics—Transactions of the ASME 70 (2), 190–199.

Keller, H.B., 1992. Numerical Methods for Two-Point Boundary Value Problems. Dover Publications, New York.

Kim, J., Swanson, S.R., 2001. Design of sandwich structures for concentrated loads. Composite Structures 52 (3–4), 365–373.

Mindlin, R.D., 1951. Influence of transverse shear deformation on the bending of classical plates. Transaction of ASME, Journal of Applied Mechanic 8, 18–31.

Noor, A.K., Burton, W.S., Bert, C.W., 1996. Computational models for sandwich panels and shells. Applied Mechanics Review 49, 155–199.

Petras, A., Sutcliffe, M.P.F., 1999. Indentation resistance of sandwich beams. Composite Structures 46 (4), 413–424.

Petras, A., Sutcliffe, M.P.F., 2000. Indentation failure analysis of sandwich beams. Composite Structures 50 (3), 311–318.

Plantema, F.J., 1966. Sandwich Construction. New York, John Wiley and Sons.

Reddy, J.N., 1984. Energy and Variational Methods in Applied Mechanics. John Wiley and Sons, Inc., New York.

Sokolinsky, V., Frostig, Y., 2000. Branching behavior in the non-linear response of sandwich panels with a transversely flexible core. International Journal of Solids and Structures 37, 5745–5772.

Sokolinsky, V.S., Frostig, Y., Nutt, S.R., 2002. Special behavior of sandwich panels with transversely flexible core under statical loading. International Journal of Non-Linear Mechanics 37 (4–5), 869–895, special issue in honor of Prof. Johann Arbocz at his retirement from the Delft University of Technology.

Sokolinsky, V.S., Shen, H., Vaikhanski, L., Nutt, S.R., 2003. Experimental and analytical study of nonlinear bending response of sandwich beams. Composite Structures 60 (2), 219–229.

Stoer, J., Bulirsch, R., 1980. Introduction to Numerical Analysis. Springer, New York.

Swanson, S.R., 1999. An examination of a high-order theory for sandwich beams. Composite Structures 44 (2–3), 169–177.

Thomsen, O.T., 1995. Theoretical and experimental investigation of local bending effects in sandwich plates. Composite Structures 30 (1), 85–101.

Thomsen, O.T., Frostig, Y., 1997. Localized bending effects in sandwich panels: photoelastic investigation versus high-order sandwich theory results. Composite Structures 37 (1), 97–108.

Vinson, J.R., 1999. The Behavior of Sandwich Structures of Isotropic and Composite Materials. Technomic Publishing Co. Inc., Lancaster.

Zenkert, D., 1995. An Introduction to Sandwich Construction. Chameleon Press Ltd., London.

Zenkert, D. (Ed.), 1997. The Handbook of Sandwich Construction, North European Engineering and Science Conference Series, EMACS, UK.